NASA Contractor Report 2938

Acoustic Emission Spectral Analysis of Fiber Composite Failure Mechanisms

Dennis M. Egan and James H. Williams, Jr.

CONTRACT NSG-3064
JANUARY 1978

NASA

NASA Contractor Report 2938

Acoustic Emission Spectral Analysis of Fiber Composite Failure Mechanisms

Dennis M. Egan and James H. Williams, Jr.

Massachusetts Institute of Technology
Cambridge, Massachusetts

Prepared for
Lewis Research Center
under Contract NSG-3064

National Aeronautics
and Space Administration

**Scientific and Technical
Information Office**

1978

INTRODUCTION

One of the major goals of researchers in acoustic emission (AE) is to be able to characterize AE sources and material failure mechanisms. AE signal characteristics such as energy, event and oscillation counts, rise and decay times, amplitude distribution, and spectral frequency distribution may be related to the strain waves which are generated by the source. Spectral frequency analysis is among the more promising techniques for assisting the characterization of AE sources.

Graphite fiber polymeric composites comprise a group of modern materials which combine high specific strength and stiffness to an extent unattainable in most conventional metals. The primary AE source mechanisms during composite deformation are (1) fracture of fiber, (2) fracture of matrix, (3) fiber-matrix debonding, (4) relaxation of fibers if they fracture, and (5) fiber pull-out against friction during composite rupture. Because some of these failure modes may be structurally more important than others and because graphite fiber polymeric composites often fail in a brittle manner, a knowledge of the source mechanism is more than academic.

The work reported here is a limited part of an overall program to study the AE characteristics of graphite fiber polymeric composites. The purpose of this paper is to illustrate the use of a particular statistical analysis procedure which may be useful in establishing quantitative AE spectral analysis measures which can distinguish specimens exhibiting

different predominant failure mechanisms, and thus distinguish the different source mechanisms.

ACOUSTIC EMISSION SPECTRAL ANALYSIS OF FIBER COMPOSITES

Review of Literature

An extensive review and summary of the literature relating to the AE monitoring of fiber composite materials and structures were conducted by Williams [1]. For the purposes of this paper, the previous work on AE spectral analysis of fiber composites will be briefly reviewed.

In observing the acoustic emission from graphite epoxy specimens, Mehan and Mullin [2] stated that acoustic events occurred in the frequency range below 20 kHz, and that each failure mechanism had a different characteristic signature. Speake and Curtis [3] reported a wide spectrum of 30-130 kHz with several intermediate discrete frequencies for notched graphite reinforced plastics and a spectrum of 0(dc)-70 kHz with intermediate discrete frequencies for waisted specimens of the same material. They observed that higher frequency components became more apparent as specimen rupture was approached but that no apparent change in the dominant frequencies occurred. When these graphite composites were subjected to torsion, specimens with type I fibers produced a broad spectrum up to 500 kHz and those with type II fibers produced frequencies up to 1 MHz. In the type I fiber composites, the dominant frequencies were in the 0-100 kHz range at twist angles less than 90° and shifted to the 100-325 kHz range for twist angles greater than 90°. It was suggested that the shift in frequency was due to either a change in the predominant failure mechanisms or changes in the specimen resonance due to the large

deformations.

Fiber fracture was reported by Mullin and Mehan [4] to have dominant frequencies at 0.6 and 3.2 kHz for high fiber volume fraction glass epoxy composites; whereas, Speake and Curtis [3] found the tensile failure of glass rovings to produce a broad-band spectrum between 0-125 kHz plus discrete frequencies at 185 and 225 kHz. Takehana and Kimpara [5] gave a spectrum of 300 Hz-20 kHz with a dip near 2 kHz for polyester reinforced with several types of glass rovings. During the pressurization phase of burst-tests of glass filament wound Polaris chambers, Green et al. [6,7] obtained a spectrum between 2 and 26 kHz.

Mehan and Mullin [2,4] further showed that different AE signatures were produced for fiber fracture, matrix fracture and debonding in boron epoxy composites and that all were in the range from 0.5-16 kHz. Low fiber volume fraction composites had discrete frequencies in the 0.6-6 kHz range with dominant frequencies at 1, 2.2 and 3 kHz, whereas high fiber volume fraction composites produced a dominant frequency of 4.7 kHz.

Pipes et al. [8] reported that the spectral content of the AE from boron aluminum composites that deformed primarily by transverse tension was unaffected by using two different transducers with a 0.1-0.3 MHz filter and a 0.1 MHz-HP filter, respectively. On the other hand, specimens that deformed with large inplane shear produced quite different spectra for the same transducer-filter substitution. We interpret these results to suggest that the AE due to transverse tension contained frequencies which were primarily in the 0.1-0.3 MHz bandwidth whereas those due to inplane shear contained significant frequencies beyond 0.3 MHz.

Reporting and Statistical Analysis

As observed in [1], the AE results contained in the AE spectral analysis literature are largely qualitative even though quantitative measures are often presented. This is primarily due to two reasons:

(1) The reporting of the AE research is often not sufficiently complete to allow quantitative comparisons of data from different sources; and

(2) Few generally accepted data analysis and interpretation techniques exist within the AE community.

The requirements suggested by the first of these reasons can be met by the adherence to an AE checklist as recommended by Williams [1]. In regards to the second reason, it should be noted that even within a single specimen, an incremental change in stress may result in a number of AE events, some of which may initiate from different sources. Thus, it is extremely unlikely that any direct comparison between a single AE event and another AE event will enable source or mechanism discrimination. Therefore, if groups of AE events are treated as random data and are statistically analyzed, it may be possible to identify group characteristics which enable source or mechanism discrimination. We believe that such an approach has not been used for AE spectral analysis of composites and it is the results of such an effort that we report in this paper.

EXPERIMENTAL EQUIPMENT, SPECIMENS AND PROCEDURES

Equipment

An FC-500 (Acoustic Emission Technology, Inc.) wide-band transducer was used. The vendor calibration of the transducer displayed a nearly flat response over the frequencies 125 kHz to 2 MHz. The transducer's sensitivity over this range was approximately -85 dB(re 1V/μ Bar). The transducer was held on the specimen with two rubber bands at a contact force of about 15N, and generally coupled with AET-SC6 viscous resin. The transducer's output was preamplified by 60 dB and bandpass filtered between 125 kHz and 2 MHz. The filter had a 24 dB/octave roll-off on each side of the passband. A signal processor (AET Model 201) provided an additional 40 dB amplification, and contained the voltage threshold setting which was generally maintained at 0.7V. Amplified AE signals were recorded on a video tape recorder (AET-modified Sony AV-3650) which exhibited a flat reproduction response between 100 kHz and 2 MHz. A spectral analyzer (Hewlett Packard Model 8557 A) was used to monitor the system's background noise during testing and to perform the AE spectral analysis. Data were recorded on an X-YY recorder (Hewlett Packard Model 7046 A). An Instron Universal Testing Machine (89,000 N rating) was used to tensile load the specimens at a displacement rate which was generally 2.15×10^{-4} m/sec.

Specimens

The study of failure mechanisms can be facilitated by the choice of specimens in which one or two such mechanisms predominate. Four types of uniaxial tensile specimens were selected: 0°, 10° and 90° unidirectional (as measured relative to the tensile loading axis), and $[\pm 45°, \pm 45°]_s$. The specimens were cut from laminates of AS-1 graphite fibers (Hercules) in a PR-288 polyimide resin (3M Co.). The fiber volume fraction was 0.52.

Spectral Analysis Procedures

AE generated just prior to each specimen's rupture were spectrally analyzed in an attempt to identify any characteristic spectral signatures. The taped records of each AE event were replayed on the video recorder as a periodic gated signal. The resulting signal was input into the spectral analyzer which was operated between 125 kHz and 1 MHz (swept at 20 kHz/sec), with a maximum resolution of 10 kHz. (No discernable data were observed above 1 MHz.)

It is important to note that each recorded AE event was actually superposed onto some level of background noise. Thus, we were motivated to attempt to separate the spectrum of the AE event from the spectrum of the background noise upon which the AE event spectrum was superposed. Assuming that an AE event and the background noise were independent random variables with no correlation, the "separation" of the AE event's spectrum from the system background noise spectrum was accomplished as suggested by Newland [9]. First, a sample of system background noise was

obtained. This noise sample was taken just prior to the AE event to be analyzed and it was taken for an equal time duration as the gated AE event. The mean square spectral density of the system background noise was generated, maintaining all the control settings the same as those used for processing the AE event plus its accompanying superposed noise. The mean square spectral density of the AE event was then obtained by substracting the system background noise spectrum from the spectrum of the AE event plus superposed noise.

Extensive details of the equipment, specimens and test procedures are given by Egan [10].

RESULTS

Fracture and Typical AE Results

Both fracture characterizations and a number of typical AE measures were obtained. These included analyses of scanning electron microscopy of the fracture surfaces, failure modes (Table 1), and ultimate loads (Table 2). Also, the time-domain character of the AE, AE oscillation and RMS counts, AE pressure excitation of the transducer, and AE shake-down (the quasi-irreversibility of AE until the previous maximum historical load has been exceeded) were investigated and are reported in detail by Egan [10].

Spectral Analysis

The normalized spectral energy distribution for each of approximately 300 AE events were computed and plotted. As indicated earlier, these AE events occurred within about 90% of the ultimate load. The spectra were normalized by dividing the area under each 10 kHz increment of the AE spectral energy density curve by the total area under the curve within the bandwidth 125 kHz - 1 MHz. Thus, the units on the ordinate were dimensionless. Each of these AE event normalized spectra has been plotted by Egan [10].

The mean normalized spectral energy distribution for each specimen was derived as the average of its individual AE event normalized spectral densities. These are given in Figs. 1 through 15 where the number of

averaged individual spectra which were used for each specimen is given also. The mean normalized spectral energy distribution is labeled #1 and curves #2 and #3 are one standard diviation from the mean. (Note that negative values were potted as zero for curve #2.)

ANALYSIS

A visual examination of Figures 1 through 15 did not suggest to us quantitative distinctions between one mean normalized spectrum and another. Therefore, each mean normalized spectrum was quantified and compared statistically using a paired-sample t test. (See, for example, [11].) In this test the differences between any two mean normalized spectra at various frequencies are calculated, and then on the basis of a computed t statistic the hypothesis that the true mean of both spectra was the same is either accepted or rejected. This may be formally summarized as follows:

Hypothesis: $(H_o: \mu_j = \mu_i)^*$ The mean normalized spectrum of specimen i and the mean normalized spectrum of specimen j both came from the same universal mean normalized spectrum. (Alternative Hypothesis — H_A: $\mu_i > \mu_j$ or $\mu_i < \mu_j$).

Level of Significance: $\alpha = 0.74$ (Type I Error)

Statistic:
$$t = \frac{\bar{X}_i - \bar{X}_j}{\sqrt{\frac{\sum_{k-1}^{N} [d_k - (\bar{X}_i - \bar{X}_j)]^2}{N(N-1)}}}$$

---

*This is, strictly speaking, a "null hypothesis".

$$\text{where } \bar{X}_{\ell} = \frac{\sum_{m=1}^{N} X_{\ell m}}{N}, \qquad d_k = X_{ik} - X_{jk}$$

N = Sample Size = 68

N-1 = Degrees of Freedom (assuming a normal population distribution)

Two-Tailed t Test: $t_{0.63}(67) = 0.33$

Reject if $t < -0.33$ or $t > 0.33$

The arithmetic universal mean is denoted by μ, and the observations (the values of the mean normalized spectra) are designated as X which are sampled at 68 different frequencies, uniformly distributed over the bandwidth between 125 kHz and 800 kHz. The choice of 0.74 as the level of significance was made after examining its impact upon the sample spectra, and thus represents an arbitrary choice which is subject to discretion.

Table 3 gives the percentage of specimen pair comparisons for which the hypothesis was accepted; the higher the number in the table, the more similar the spectra. With the exception of 0° - 0° comparisons, like-specimen comparisons result in a higher percentage of hypothesis acceptances than unlike-specimen comparisons. The 0° - 0° exception might be related to the relatively large scatter in the 0° specimens' rupture loads as shown in Table 2.

CONCLUSIONS AND RECOMMENDATIONS

A program to investigate the acoustic emission of graphite fiber polyimide composite failure mechanisms has been conducted. Although a number of AE measures has been investigated, AE spectral energy analysis has been studied extensively with an emphasis on the statistical distinction of AE which were generated by different types of composites and thus different types of fracture mechanisms.

Because of the high improbability that direct comparison of individual AE events can result in quantitative source discrimination measures, individual AE event spectral densities were combined to derive mean normalized spectral densities for each specimen. Furthermore, visual inspection of even the specimen mean normalized spectral densities suggests little regarding quantitative distinctions. A paired-sample t statistical comparison of mean normalized spectral energy distributions appears to provide quantitatives discrimination between the AE from 10°, 90° and $[\pm 45°, \pm 45°]_s$ specimens. For the limited experimental data obtained, the paired-sample t test could not achieve either conclusive distinction or unique recognition of the AE from 0° specimens.

Because of the encouraging results which have been presented, we recommend that more statistical characterizations of AE spectra be performed. This would include the analysis of more AE events to obtain better estimates of the mean normalized spectra, and the use of other types of statistical comparative tests. Also, the composite dispersion and

attentuation characteristics should be studied in order to develop a better understanding of the propagation effects on the spectra and amplitudes of AE signals.

REFERENCES

1. J.H. Williams, Jr., "Acoustic Emission Monitoring of Fiber Composite Materials and Structures", Artech No. J7600.33. Prepared for David Taylor Naval Ship R & D Center, February 1977.

2. R.L. Mehan and J.V. Mullin, "Analysis of Composite Failure Mechanisms Using Acoustic Emissions", J. Composite Materials, Vol. 5, April 1971, pp. 266-269.

3. J.H. Speake and G.J. Curtis, "Characterization of the Fracture Processes in CFRP using Spectral Analysis of the Acoustic Emissions Arising from the Application of Stress", International Conference on Carbon Fibers, London, February 1974. The Plastics Institution, Paper No. 29.

4. J.V. Mullin and R.L. Mehan, "Evaluation of Composite Failures through Fracture Signal Analysis", J. Testing and Evaluation, Vol. 1, No. 3, May 1973, pp. 215-219.

5. M. Takehana and I. Kimpara, "Internal Fracture and Acoustic Emission of Fiberglass Reinforced Plastics", Department of Naval Architecture, University of Tokyo, Tokyo, Japan.

6. A.T. Green, C.S. Lockman and R.K. Steele, "Acoustic Verification of Structural Integrity of Polaris Chambers", Modern Plastics, Vol. 41, No. 11, July 1964, pp. 137-139, 178 and 180.

7. C.R. Morais and A.T. Green, "Establishing Structural Integrity Using Acoustic Emission", Monitoring Structural Integrity Using Acoustic Emission, ASTM STP 571, 1975, pp. 184-199.

8. R.B. Pipes, N.J. Ballintyn and W.R. Scott, "Acoustic Emission Response of Metal Matrix Composites", Naval Air Development Center Report No. NADC-76082-30, January 1976.

9. D.E. Newland, Random Vibrations and Spectral Analysis, Longmans Group, Ltd., London, 1975, pp. 67-73.

10. D.M. Egan, "Acoustic Emission Analysis of Fiber Composite Failure Mechanisms", S.M. and O.E. Thesis, Massachusetts Institute of Technology, May 1977.

11. I. Miller and J.E. Freund, Probability and Statistics for Engineers, Prentice Hall, Inc., Englewood Cliffs, New Jersey, 1965. pp. 165-170.

Table 1

Fracture Modes of Graphite Fiber Polyimide Composite Specimens

Specimen Type	Fracture Mode
0° (Unidirectional)	Fiber fracture, fiber-matrix debonding with fiber pullout, shear fracture of matrix, and tensile fracture of matrix.
10° (Unidirectional)	Intralaminar shear fracture of matrix.
90° (Unidirectional)	Tensile fracture of matrix.
$[\pm 45°, \pm 45°]_s$	Shear and tensile intralaminar fracture of matrix followed by delamination and fiber fracture.

Table 2

Summary of Mean and Standard Deviation of Ultimate Loads

Specimen Type (Four specimens each type)	Mean Ultimate Load (kN)	Standard Deviation (kN)	Parameter of Scatter (Std. Dev./Mean)
0°	20.672	6.1170	0.2959
10°	6.664	0.2249	0.0337
90°	0.831	0.0887	0.1068
$[\pm 45°, \pm 45°]_s$	2.310	0.0796	0.0345

All cross-sectional dimensions were 12.7×10^{-3} m by 1×10^{-3} m.

Table 3

Summary of Paired-Sample t Statistics
over 125 kHz-800 kHz Bandwidth

	0°	10°	90°	$[\pm 45°, \pm 45°]_s$
0°	16.7	25.0	31.2	56.2
10°	25.0	66.7	50.0	50.0
90°	31.2	50.0	66.7	56.2
$[\pm 45°, \pm 45°]_s$	56.2	50.0	56.2	83.3

Table gives the percentage of specimen comparisons for which the stated hypothesis was accepted.

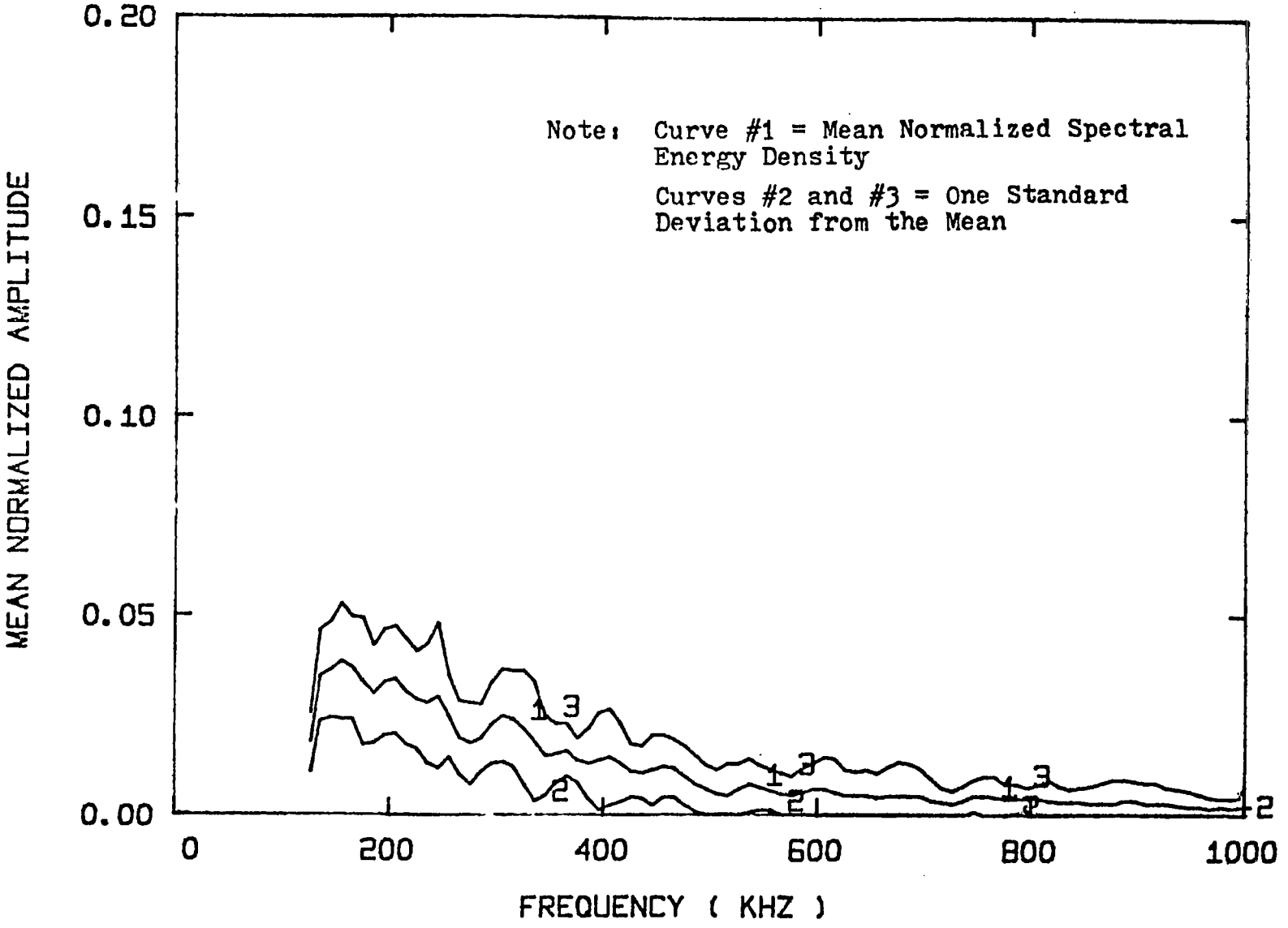

Fig. 1 Mean normalized spectral energy density for 0° specimen No. 1. (Number of individual averaged spectra = 16.)

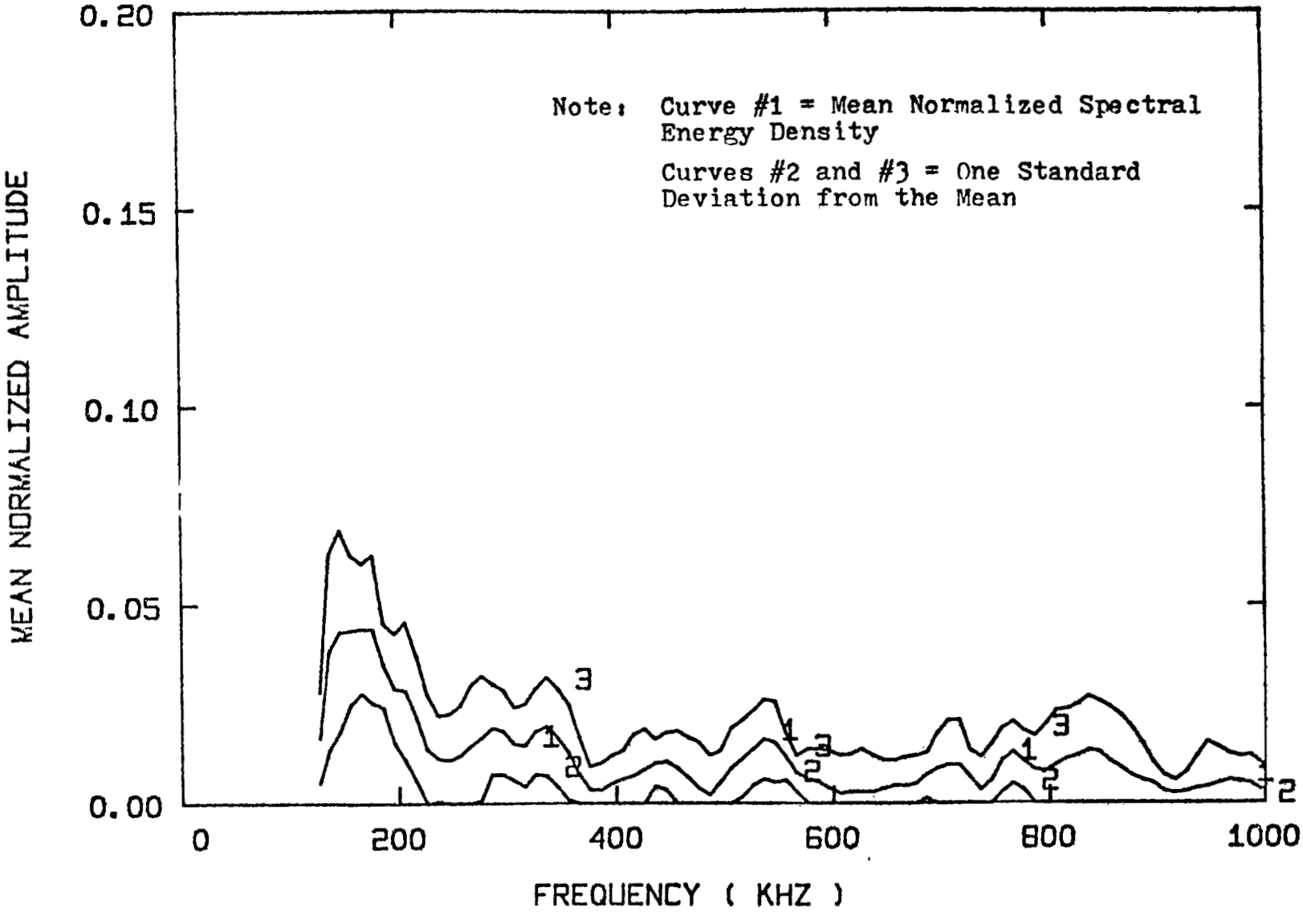

Fig. 2 Mean normalized spectral energy density for 0° specimen No. 2. (Number of individual averaged spectra = 19.)

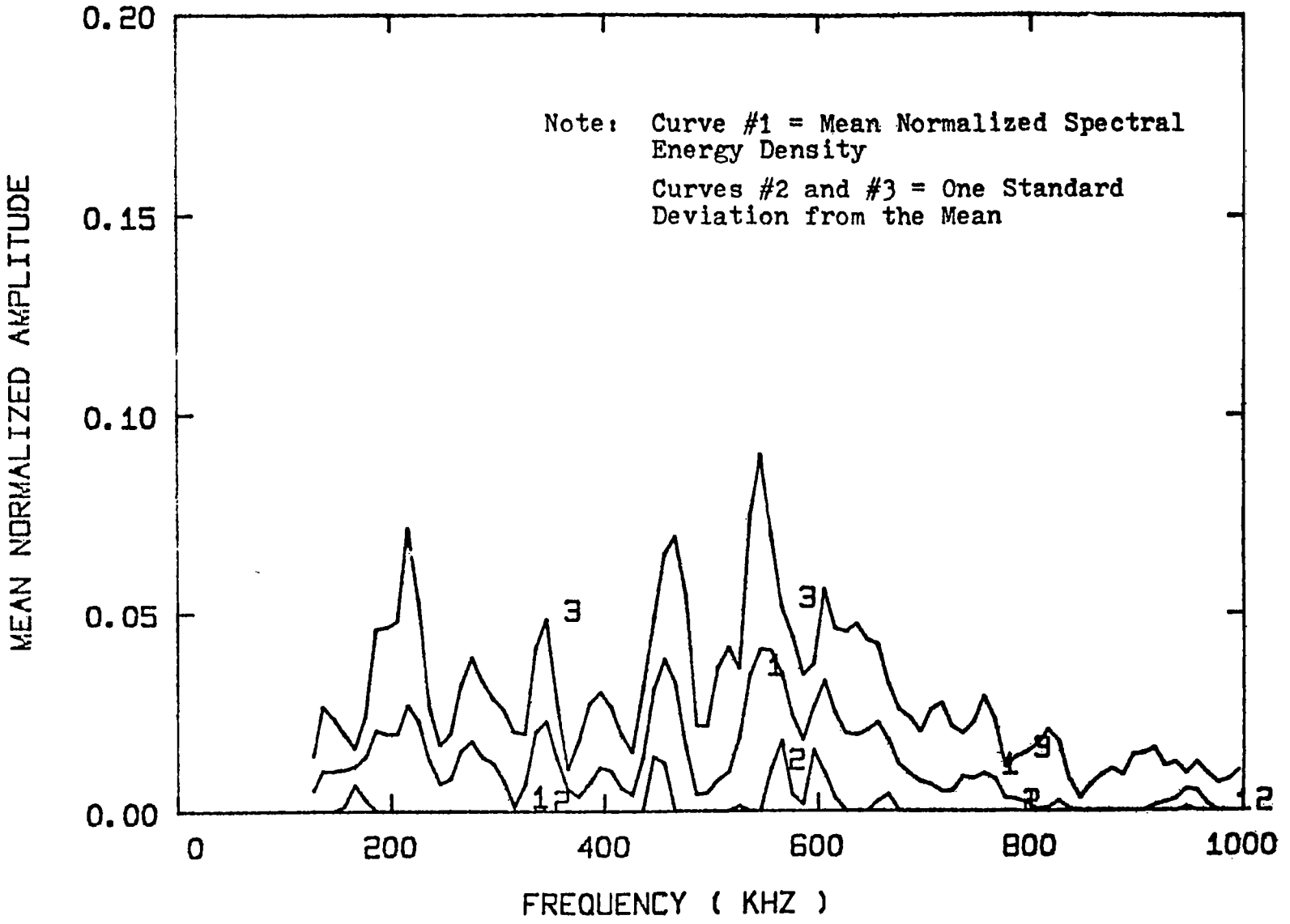

Fig. 3 Mean normalized spectral energy density for 0° specimen No. 3. (Number of individual averaged spectra = 12.)

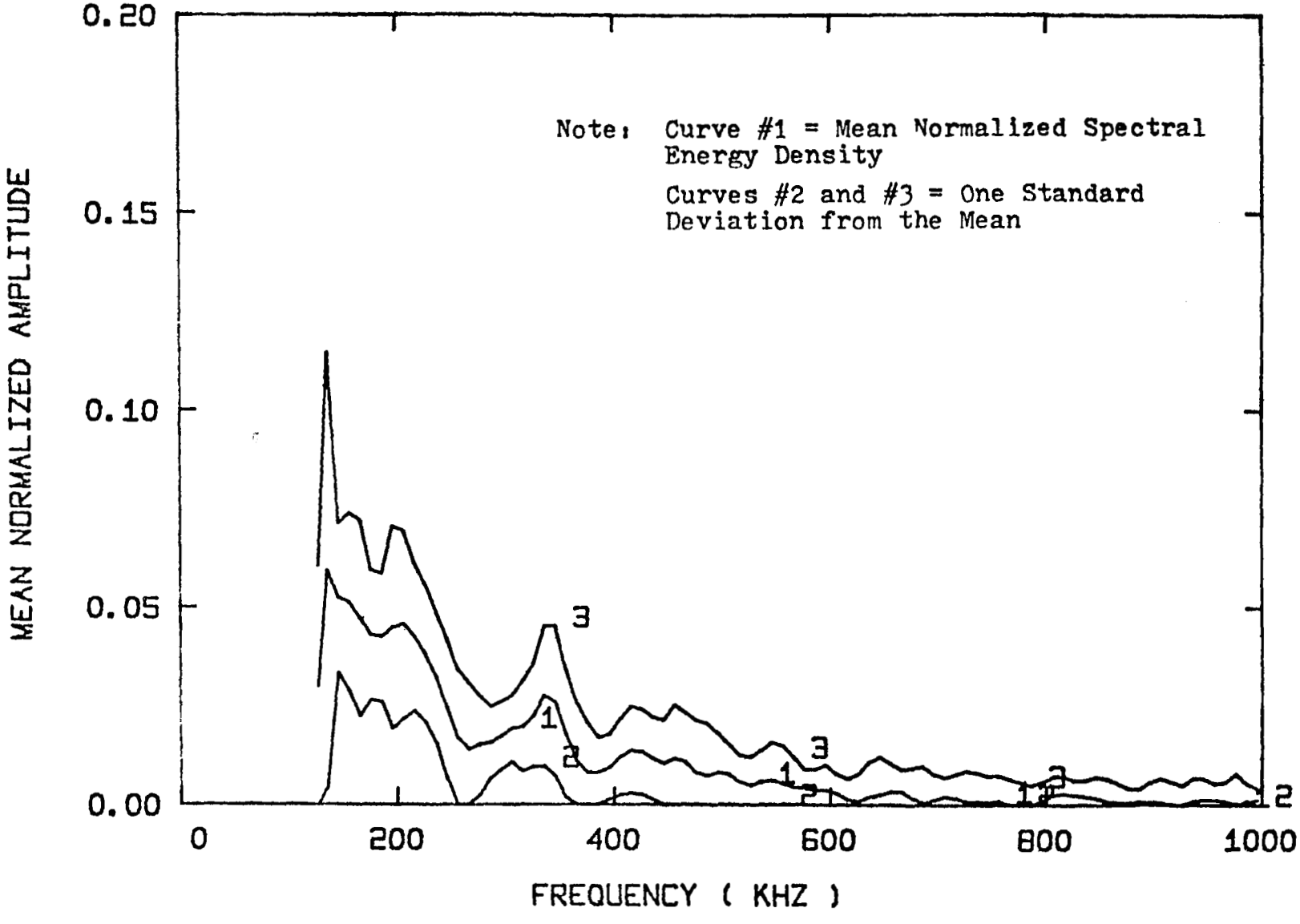

Fig. 4 Mean normalized spectral energy density for 0° specimen No. 4. (Number of individual averaged spectra = 23.)

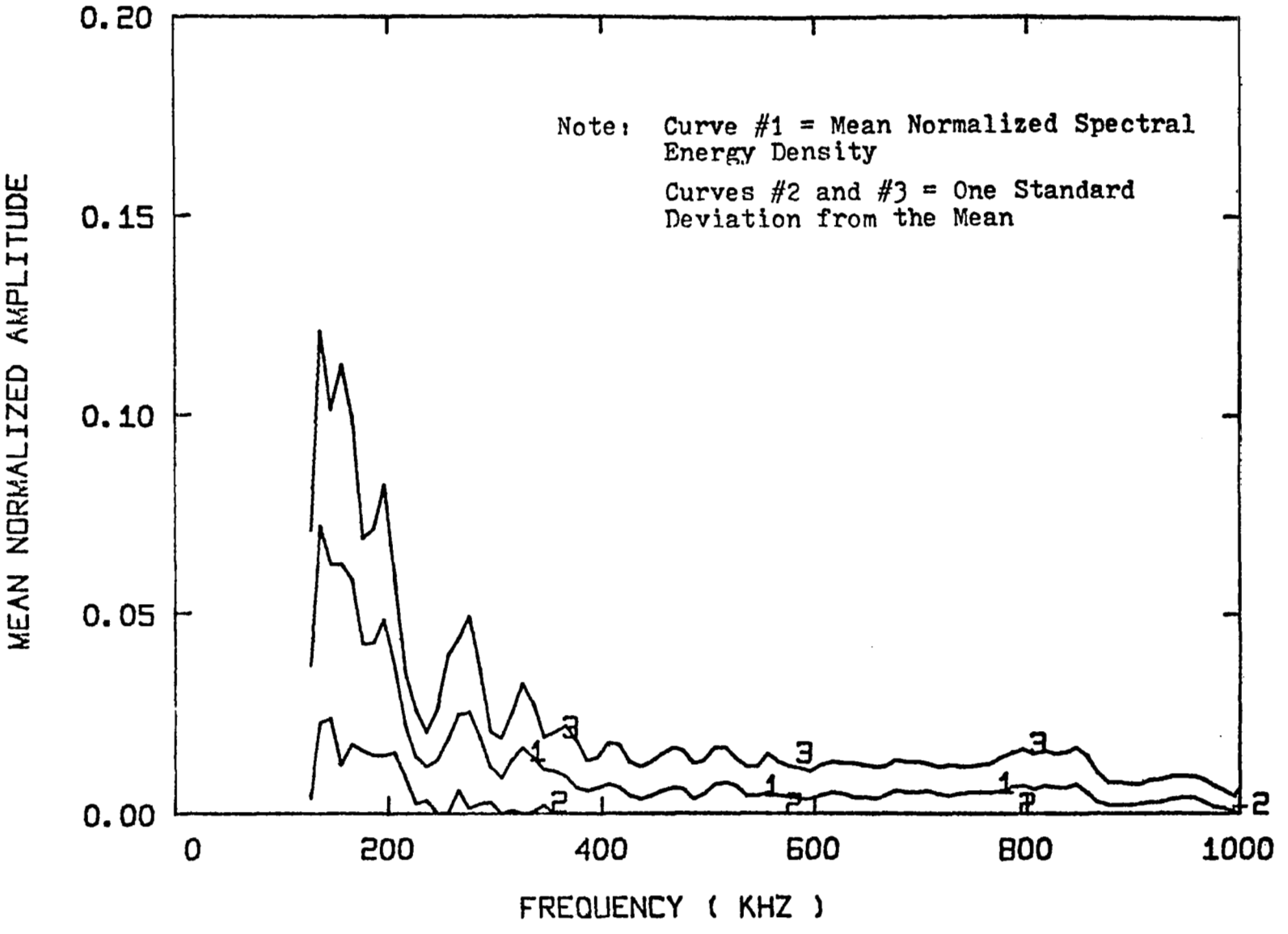

Fig. 5 Mean normalized spectral energy density for 10° specimen No. 1. (Number of individual averaged spectra = 33.)

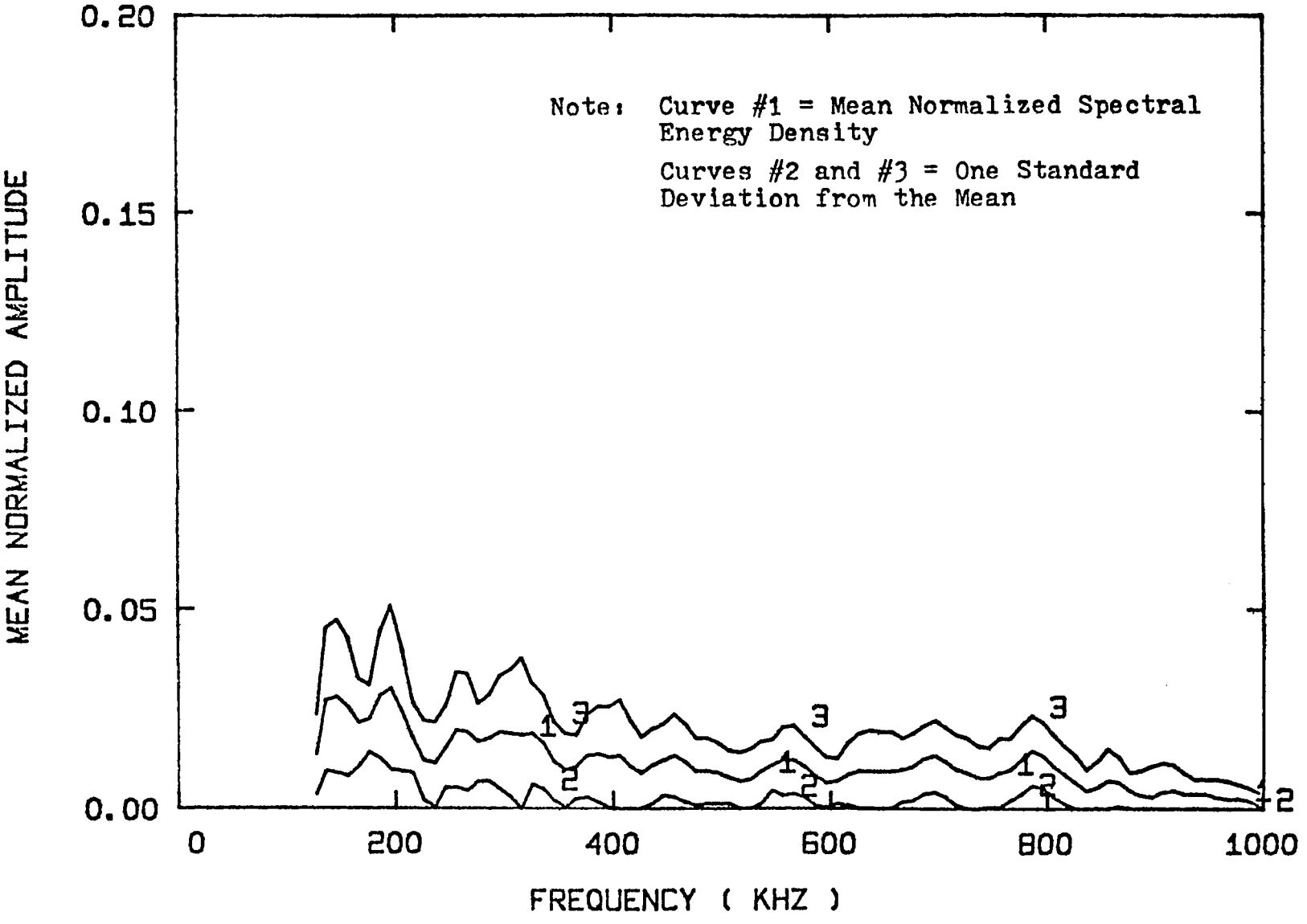

Fig. 6 Mean normalized spectral energy density for 10° specimen No. 2. (Number of individual averaged spectra = 20.)

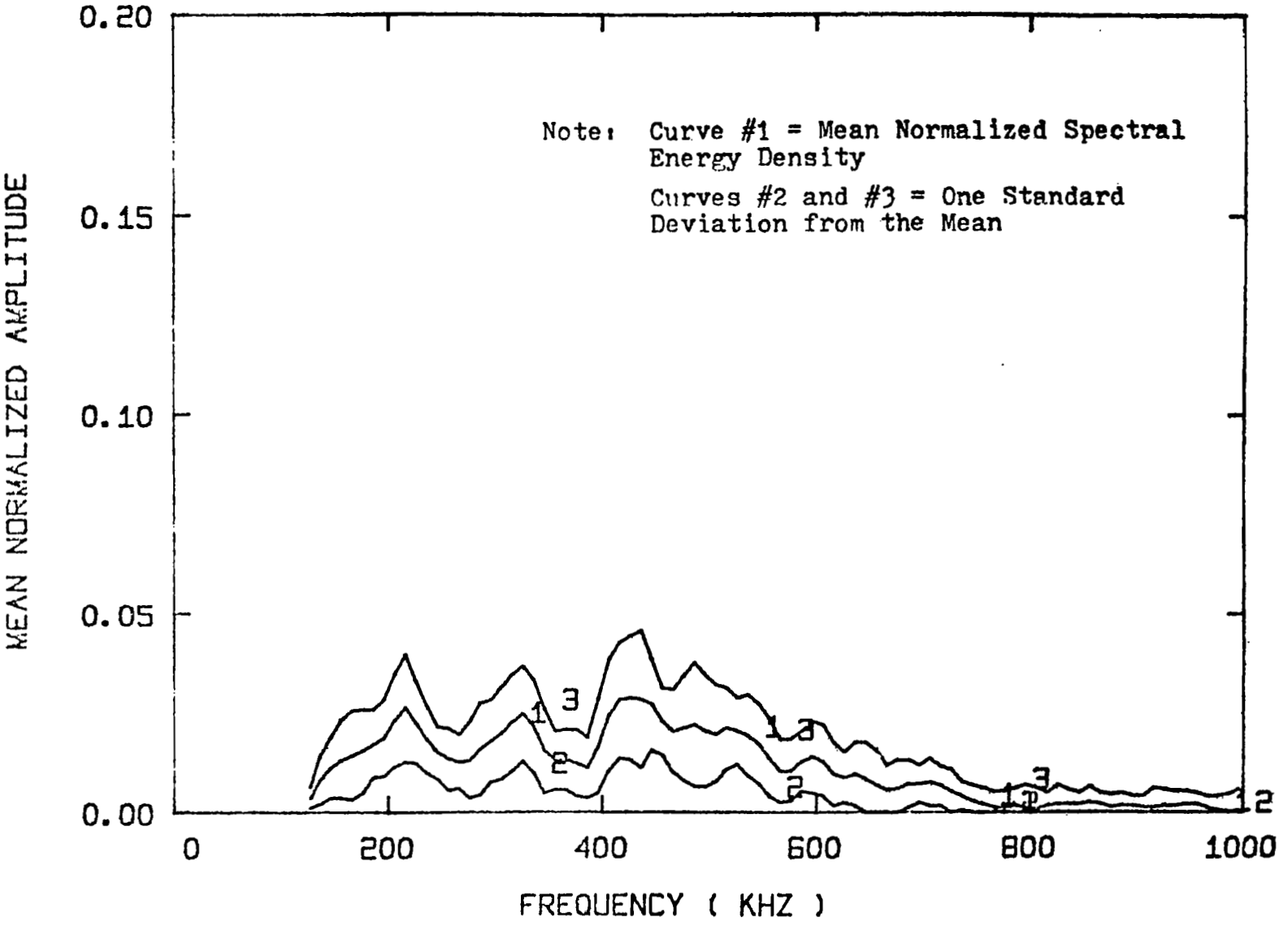

Fig. 7 Mean normalized spectral energy density for 10° specimen No. 3. (Number of individual averaged spectra = 26.)

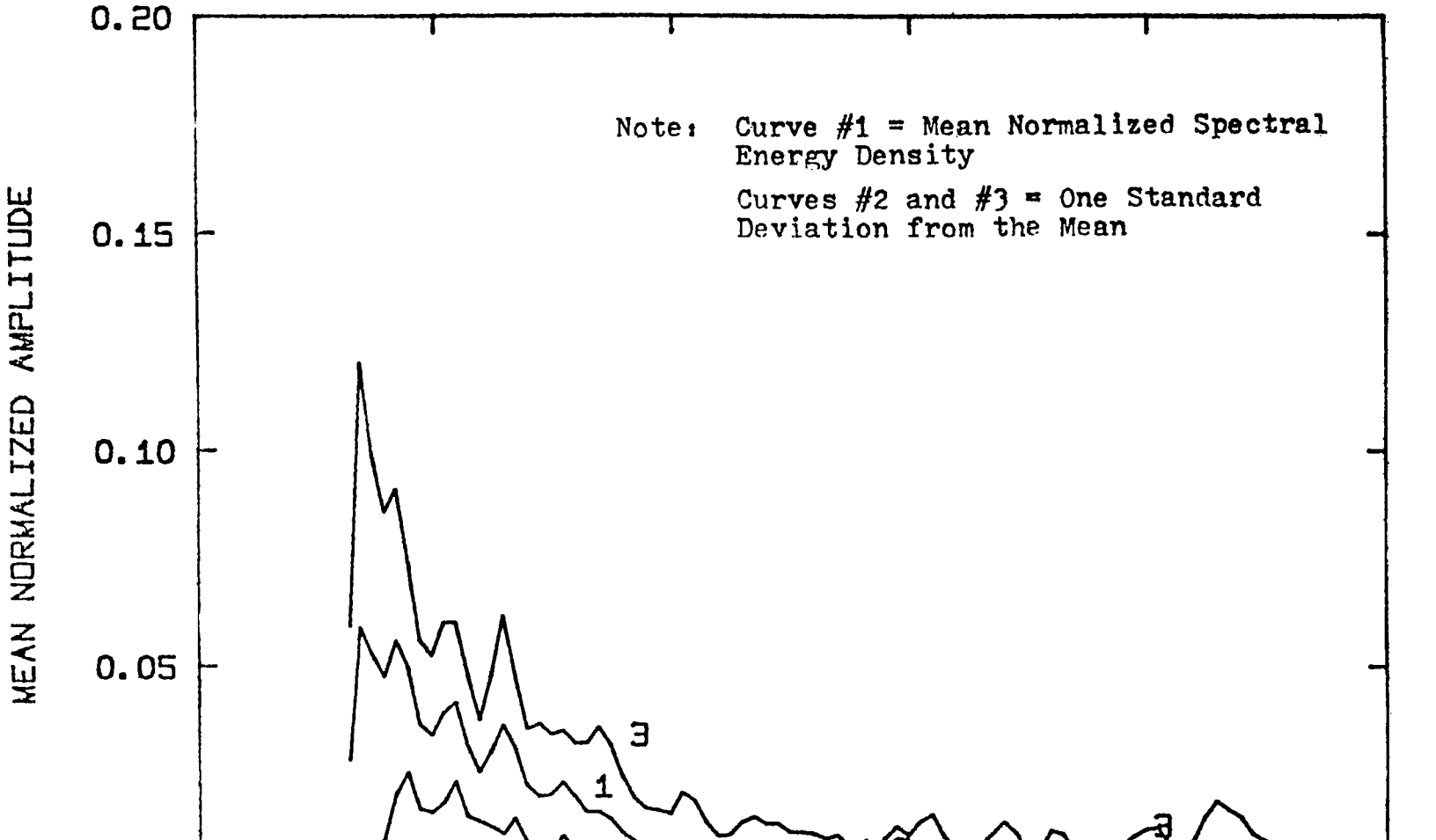

Fig. 8 Mean normalized spectral energy density for 90° specimen No. 1. (Number of individual averaged spectra = 14.)

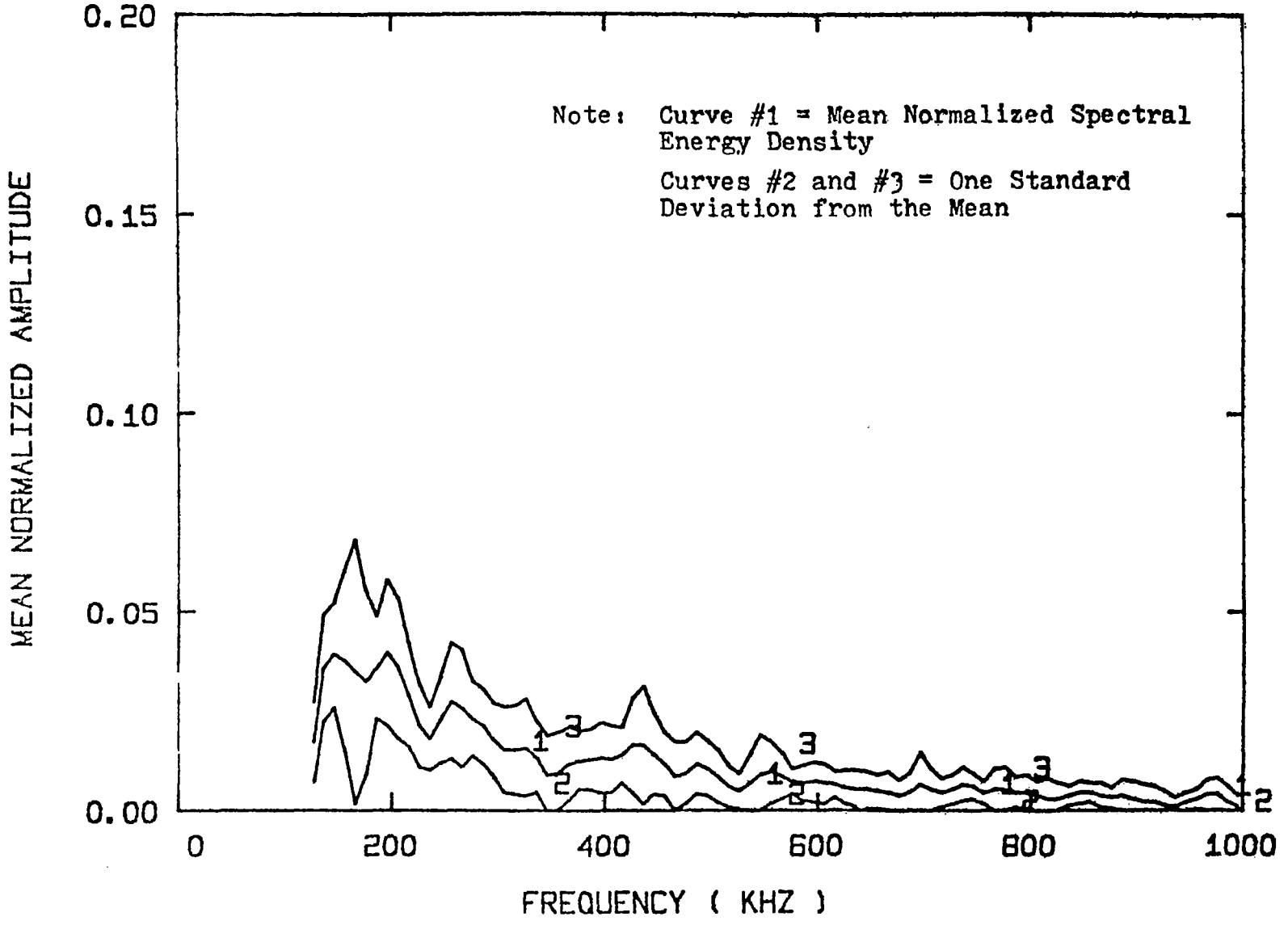

Fig. 9 Mean normalized spectral energy density for 90° specimen No. 2. (Number of individual averaged spectra = 10.)

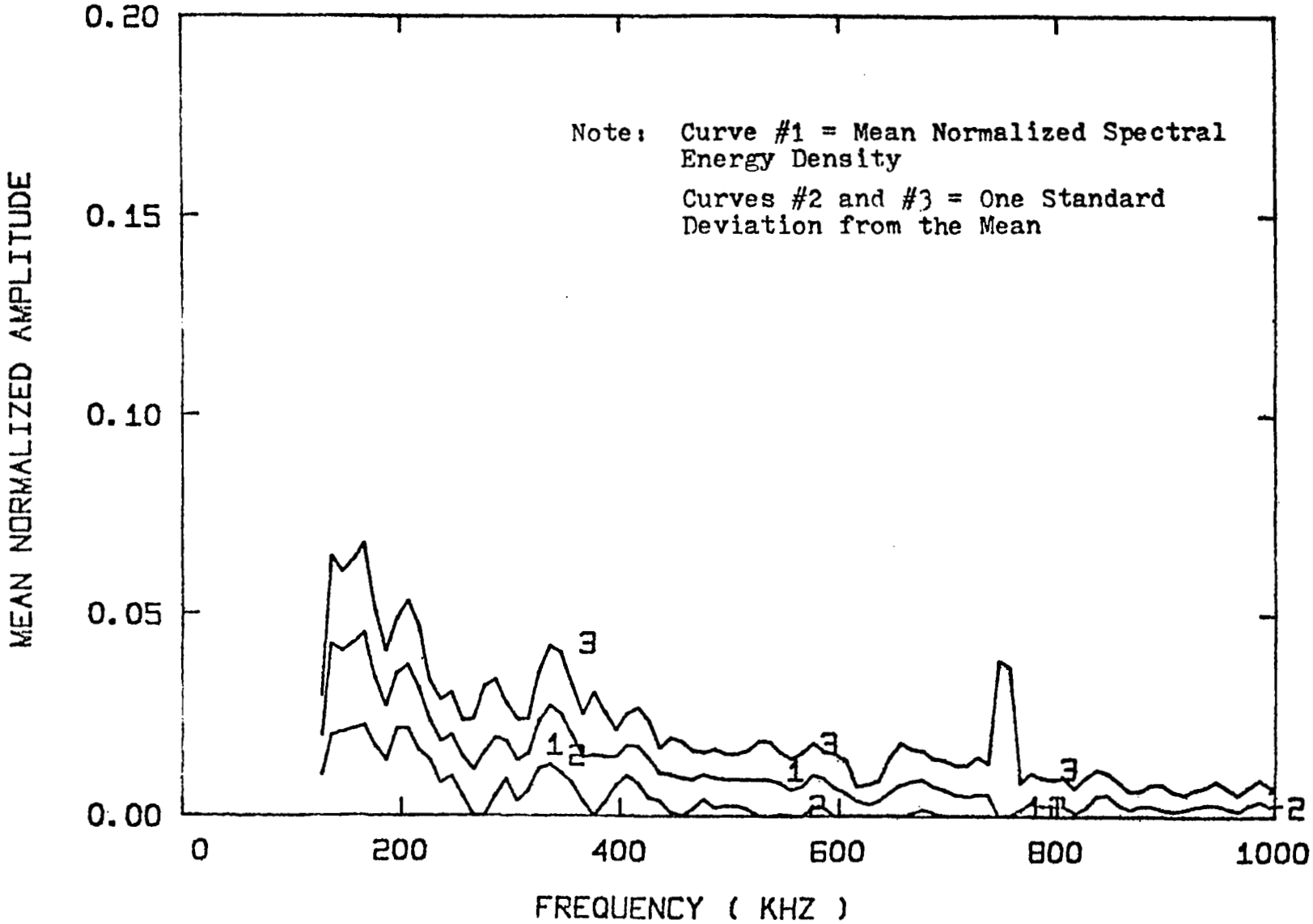

Fig. 10 Mean normalized spectral energy density for 90° specimen No. 3. (Number of individual averaged spectra = 14.)

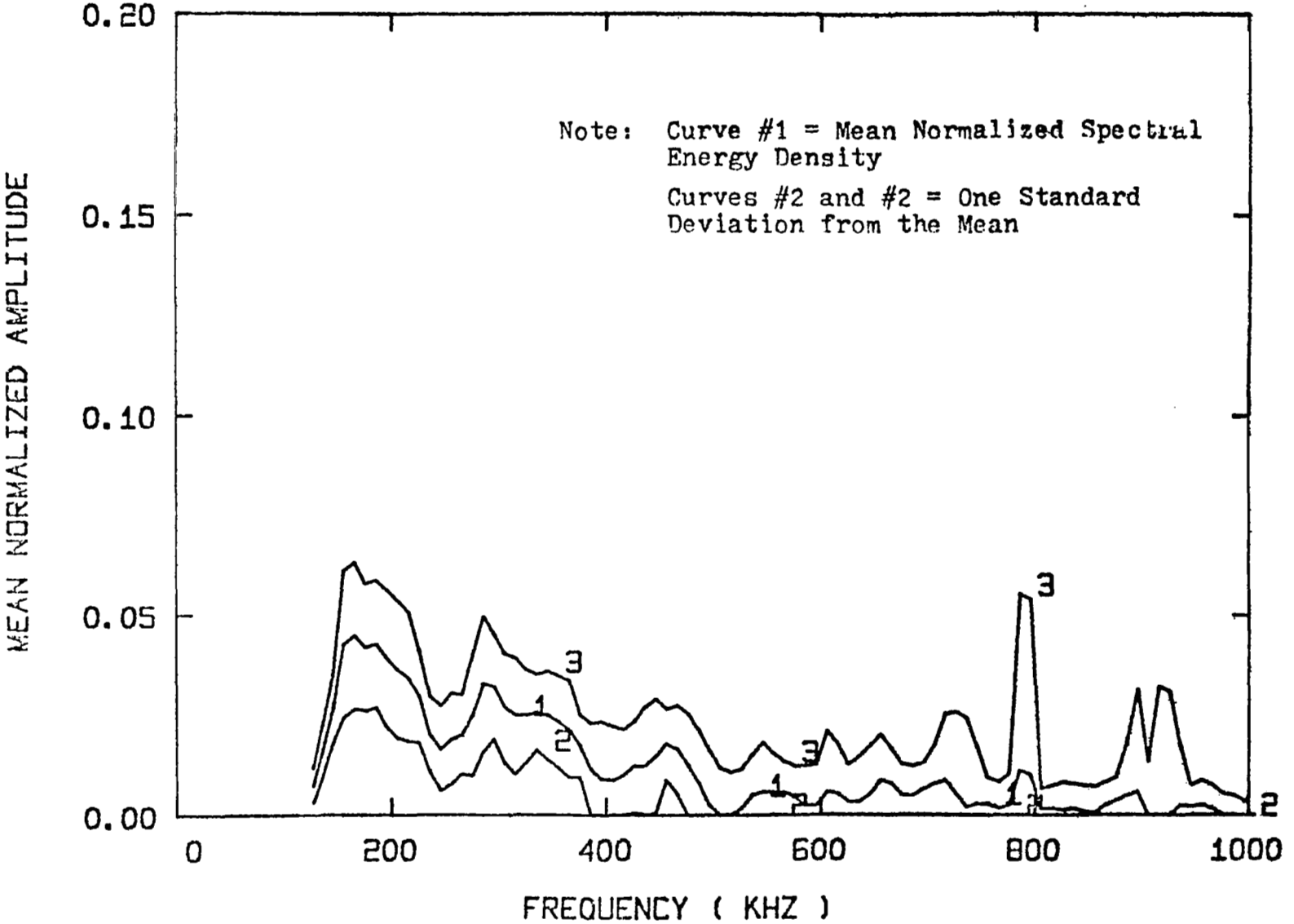

Fig. 11 Mean normalized spectral energy density for 90° specimen No. 4. (Number of individual averaged spectra = 29.)

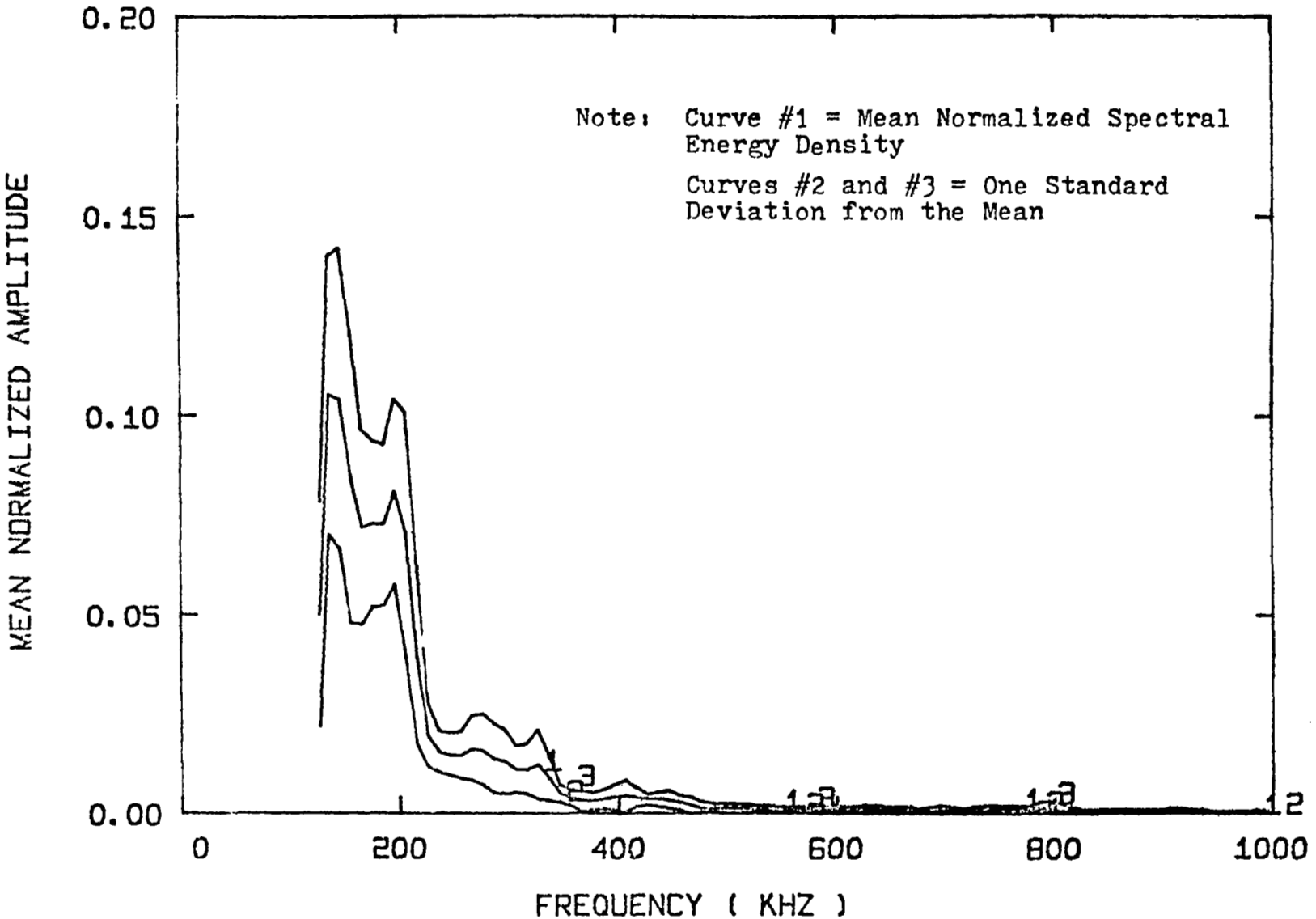

Fig. 12 Mean normalized spectral energy density for $[\pm 45°, \pm 45°]_s$ specimen No. 1. (Number of individual averaged spectra = 19.)

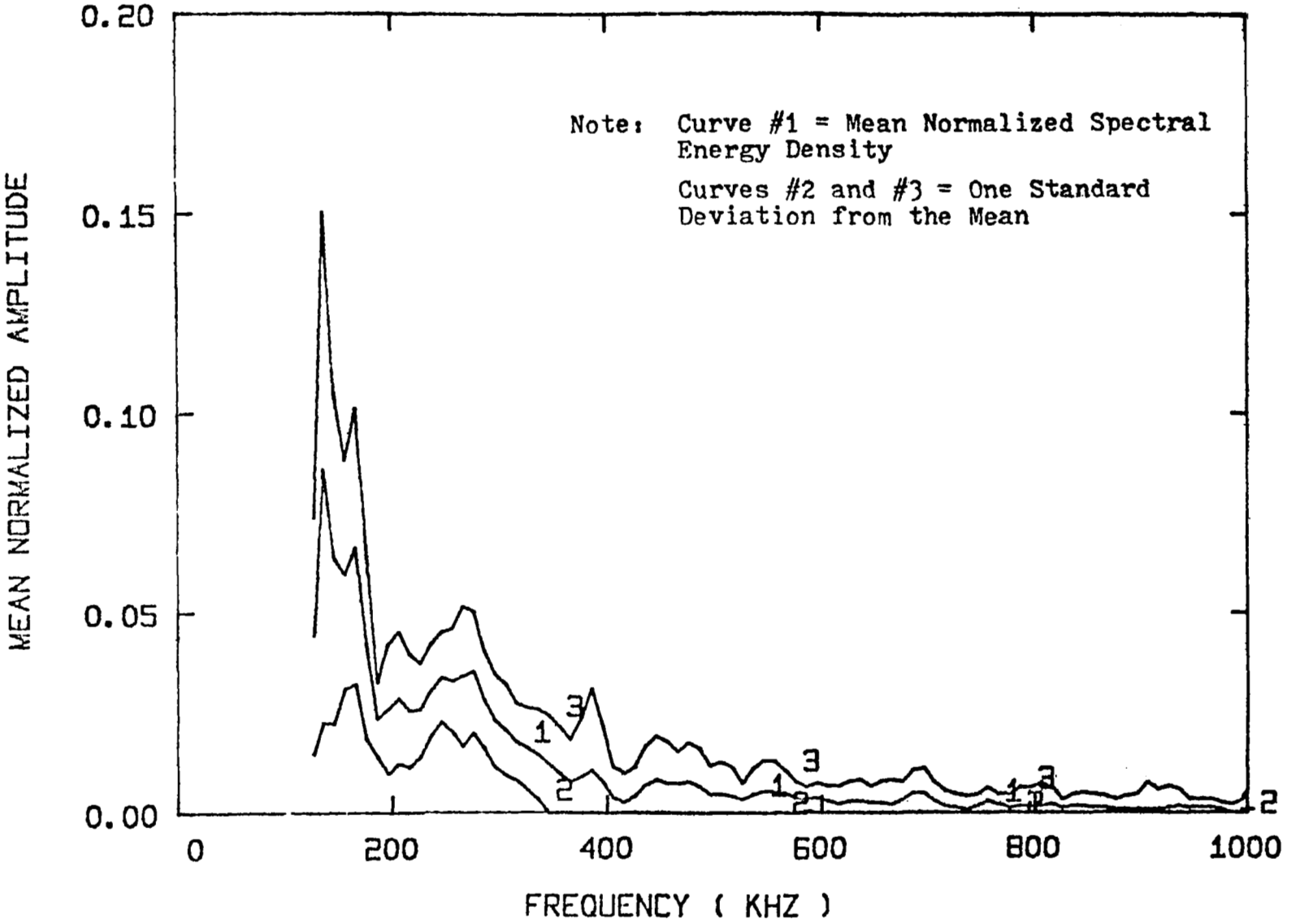

Fig. 13 Mean normalized spectral energy density for $[\pm 45°, \pm 45°]_s$ specimen No. 2. (Number of individual averaged spectra = 19.)

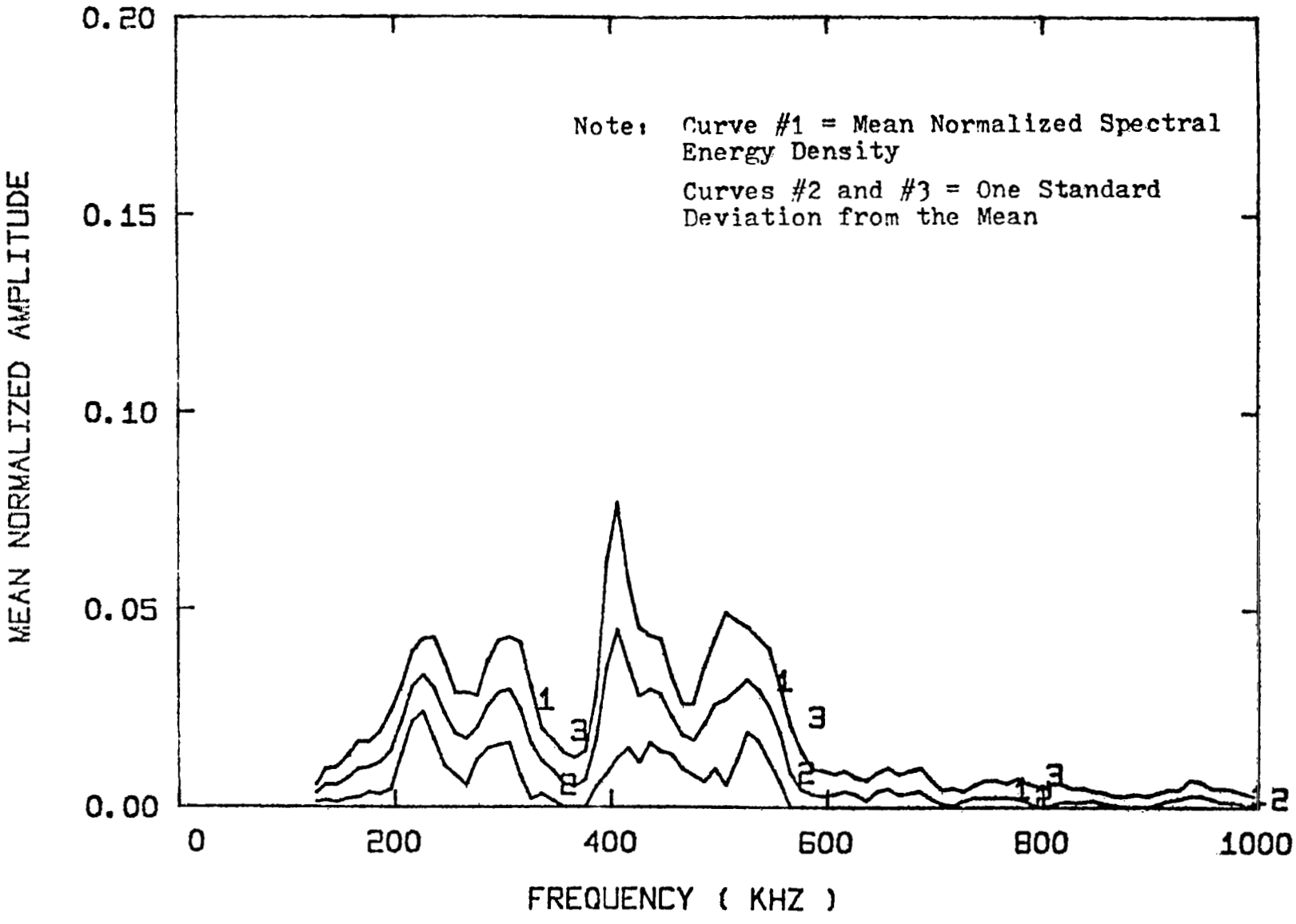

Fig. 14 Mean normalized spectral energy density for $[\pm 45°, \pm 45°]_s$ specimen No. 3. (Number of individual averaged spectra = 15.)

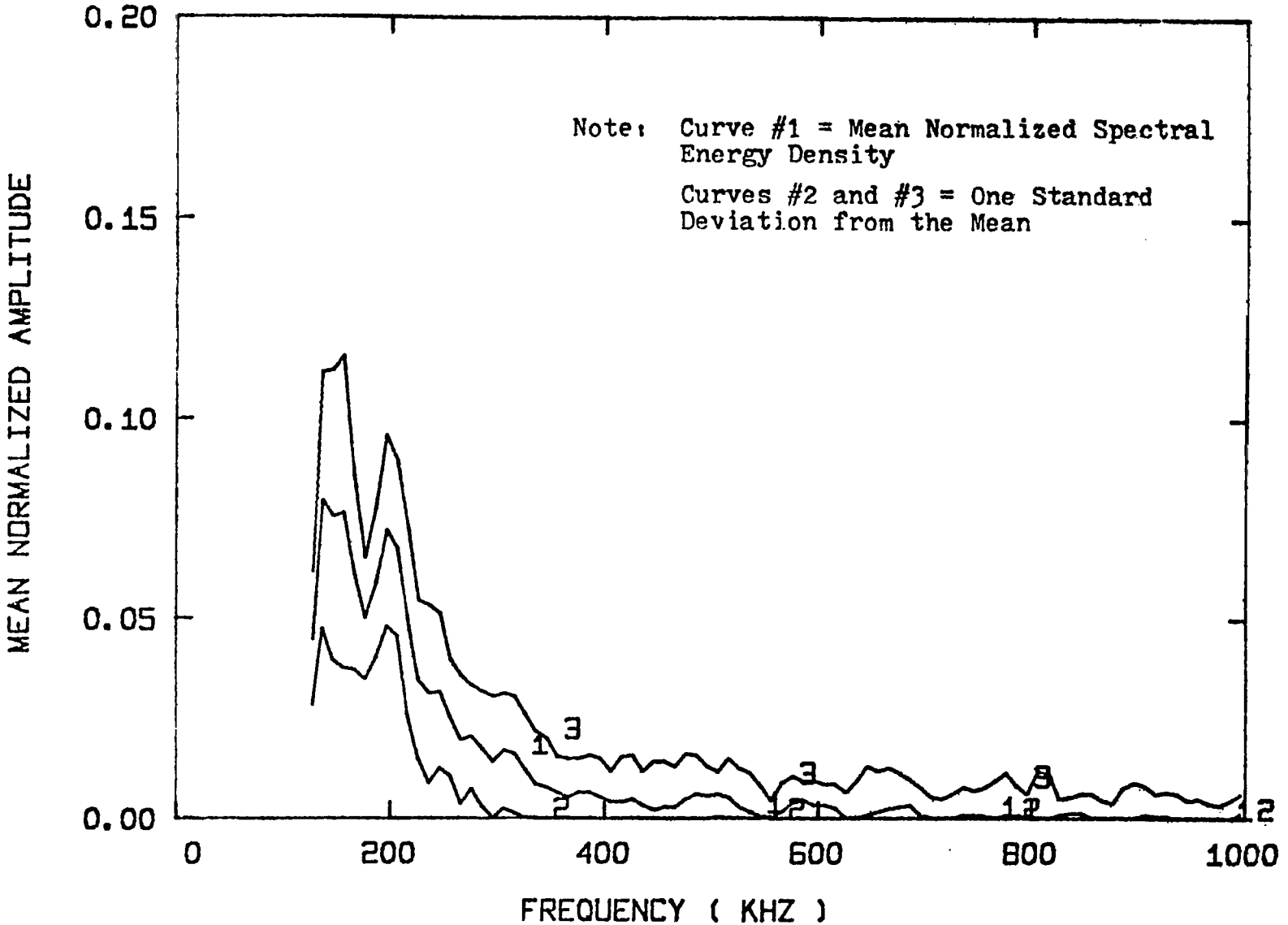

Fig. 15 Mean normalized spectral energy density for $[\pm 45°, \pm 45]_s$ specimen No. 4. (Number of individual averaged spectra = 22.)

1. Report No.	2. Government Accession No.	3. Recipient's Catalog No.
NASA CR-2938		

4. Title and Subtitle	5. Report Date
ACOUSTIC EMISSION SPECTRAL ANALYSIS OF FIBER COMPOSITE FAILURE MECHANISMS	January 1978
	6. Performing Organization Code
7. Author(s)	8. Performing Organization Report No.
Dennis M. Egan and James H. Williams, Jr.	None
	10. Work Unit No.
9. Performing Organization Name and Address	
Massachusetts Institute of Technology Cambridge, Massachusetts 02139	11. Contract or Grant No. NSG-3064
	13. Type of Report and Period Covered
12. Sponsoring Agency Name and Address	Contractor Report
National Aeronautics and Space Administration Washington, D.C. 20546	14. Sponsoring Agency Code

15. Supplementary Notes

Final report. Project Manager, Alex Vary, Materials and Structures Division, NASA Lewis Research Center, Cleveland, Ohio 44135

16. Abstract

A program to investigate the acoustic emission of graphite fiber polyimide composite failure mechanisms with emphasis on frequency spectrum analysis is described. Although visual examination of spectral densities could not distinguish among fracture sources, a paired-sample t statistical analysis of mean normalized spectral densities did provide quantitative discrimination among acoustic emissions from 10°, 90°, and $[\pm 45^{\circ}, \pm 45^{\circ}]_{S}$ specimens. Comparable discrimination was not obtained for 0° specimens.

17. Key Words (Suggested by Author(s))	18. Distribution Statement
Acoustic emission Composite materials Nondestructive testing	Unclassified - unlimited STAR Category 24

19. Security Classif. (of this report)	20. Security Classif. (of this page)	21. No. of Pages	22. Price*
Unclassified	Unclassified	34	A03

* For sale by the National Technical Information Service, Springfield, Virginia 22161

NASA-Langley, 1978